Stability of dimesons

J. Carlson and L. Heller
Theoretical Division, Los Alamos National Laboratory, Los Alamos, New Mexico 87545

J. A. Tjon
Institute for Theoretical Physics, P.O. Box 80.006, 3508 TA Utrecht, The Netherlands
(Received 31 August 1987)

Using only the known short-distance behavior of quantum chromodynamics it is possible to prove that, for sufficiently large quark mass m, and fixed antiquark mass, the dimeson $(Q^2\bar{q}^2)$ must be stable against strong decay into two mesons. The binding energy is $\frac{1}{9}m\alpha_s^2[1+O(m^{-1})]$. We then study systems in which Q is c or b, using the many-body confining interaction that comes from a Born-Oppenheimer approximation to the MIT bag model. The calculations were performed using the Green's-function Monte Carlo method. The 1^+ isoscalar dimeson $T(bb\bar{u}\bar{d})$ is bound by ~ 70 MeV with respect to two B mesons; it can only decay weakly, therefore. The calculations of the dimesons $(cc\bar{q}\,\bar{q}')$ and $(bc\bar{q}\,\bar{q}')$ are more uncertain, but indicate that the latter may also be bound.

I. INTRODUCTION

One of the important topics in particle and nuclear physics is the role of the color degree of freedom. Only limited information about this question can be obtained from ordinary mesons and baryons because there is only one color-singlet state available to the $q\bar{q}$ and q^3 systems. The simplest system for which color is a dynamical variable consists of two quarks and two antiquarks, which can exist in two independent color-singlet states.

Knowledge of the color variable can provide interesting information about the state of the system by comparison with two separated mesons, which are both in color-singlet states. In the color basis that we work in this corresponds to probability $\frac{2}{3}$ for the $(6\bar{6})$ state and probability $\frac{1}{3}$ for the $(\bar{3}3)$ state. We shall later see a four-quark bound state in which these numbers are approximately $\frac{1}{4}$ and $\frac{3}{4}$, respectively, indicating a large departure of the color wave function from that of two noninteracting mesons. The relation between these color probabilities and the masses of the quarks is a central theme of the present work.

In a number of papers[1-6] it has been suggested that the dimeson $(Q^2\bar{q}\,\bar{q}')$ is stable against breakup into the two mesons $(Q\bar{q})+(Q\bar{q}')$ provided the mass m of Q is large. Since some of these papers make purely phenomenological assumptions about the nature of the interaction in the four-quark system, the physical basis for the result is not obvious. We have recently argued[6] that for sufficiently large m the dimeson *must* be bound, and in Sec. II we show how this result follows from minimal assumptions that are consistent with quantum chromodynamics.

The bulk of the present paper is concerned with the search for bound dimesons in which the light particles are either $\bar{u}$ or $\bar{d}$, and the heavy particles c or b. [In Ref. 6 there was a similar study in which all four quarks are heavy, e.g., $(t^2\bar{c}^2)$, which is indeed expected to be bound.] There are new physics questions that arise when light quarks are considered. First of all, is the potential energy that we use, which was derived from a Born-Oppenheimer approximation to the MIT bag model,[7] valid when some of the quarks are light? One aspect of this question applies to any potential model, and that is whether or not there are important nonstatic corrections to the confining part of the potential for rapidly moving quarks. In the present paper we assume that the same potential that we used for heavy quarks[7,8] applies for light quarks as well. The details of the potential are discussed in Sec. III. Since the light quarks are relativistic we use $\sum_i (p_i^2+m_i^2)^{1/2}$ as the kinetic energy operator, and our Green's-function Monte Carlo method for solving the four-body two-channel Schrödinger equation is described in Sec. IV. The results are presented in Sec. V, and summarized in Sec. VI. The hyperfine interaction is discussed in an Appendix.

II. THE LARGE-MASS LIMIT

We want to show that, independent of the detailed nature of the confining interaction, the potential energy

$$V = V_{\text{Coulomb}} + V_{\text{confining}} \tag{2.1}$$

leads to a bound dimeson for sufficiently large quark mass if the masses of the antiquarks are held fixed. The Coulomb potential is given by

$$V_{\text{Coulomb}} = \sum_{i>j} \alpha_s \frac{F_i \cdot F_j}{r_{ij}} , \tag{2.2}$$

where F_i is the color SU(3) generator for the ith particle and α_s is the strong coupling constant. Spin-dependent terms arising from one-gluon exchange are omitted for now since their presence does not affect the conclusion.

The only assumption we need make about the confining potential is the trivial one that it remains finite when two particles come close together. In particular, we do *not* assume that it can be written as a sum of two-body potentials; indeed, such an assumption would violate theoretical expectations as well as produce unphysical van der Waals forces between hadrons.

The essential ingredient for the proof is the fact that the Coulomb potential between two quarks in a color $\bar{3}$ state is attractive, since $F_i \cdot F_j$ has the value $-\frac{2}{3}$ in that state. As the mass of those quarks increases they come closer together under the influence of that attraction and their relative wave function becomes hydrogenic with a Bohr radius a corresponding to a reduced mass $m/2$ and a coupling constant $2\alpha_s/3$:

$$a = \frac{3}{m\alpha_s} . \tag{2.3}$$

The energy associated with the QQ subsystem, therefore, is

$$E(Q^2) = -\tfrac{1}{9} m \alpha_s^2 . \tag{2.4}$$

The key point is that none of the other energies in the four-body system are proportional to m since all the other relative momenta involve antiquarks whose masses are fixed. Consequently,

$$E(Q^2 \bar{q}\, \bar{q}\,') = -\tfrac{1}{9} m \alpha_s^2 [1 + O(m^{-1})] . \tag{2.5}$$

Furthermore, the last mentioned argument about the other energies being bounded in the large-m limit applies equally well to the individual mesons $(Q\bar{q})$ and $(Q\bar{q}\,')$. In this limit, therefore,

$$E(Q\bar{q}) + E(Q\bar{q}\,') - E(Q^2 \bar{q}\, \bar{q}\,') = \tfrac{1}{9} m \alpha_s^2 [1 + O(m^{-1})] , \tag{2.6}$$

which proves that for sufficiently large m the dimeson must be bound. A logarithmic reduction in α_s as m increases, due to asymptotic freedom, does not alter this conclusion.

Note that the argument for stability presented above would fail if one or both of the antiquarks has the same mass as the quarks, as, for example, in the equal-mass case $(Q^2\bar{Q}^2)$. In such a system all relative momenta are comparable, and since the Coulomb attraction between Q and $\bar{Q}$ in the color-singlet state is twice as strong as that between Q and Q in the $\bar{3}$ state, the $Q\bar{Q}$ pairing is the preferred one. While this does not prove that there is no bound dimeson for this system, it is consistent with the fact that we have not found any.[6]

III. THE HAMILTONIAN

To derive the static potential energy for a system of quarks from the Born-Oppenheimer approximation to the MIT bag model, one is supposed to solve for the glue field and the correct bag surface for every set of positions of the quarks. The surface is deformed, in general, but it was shown in Ref. 7 that when all the quark separations are comparable and $\lesssim 1$ fm, a spherical approximation to the bag is adequate. Making a dipole approximation to the homogeneous part of the Green's function for a sphere yields[7]

$$V_S^{(N)} = \alpha_s \sum_{i>j}^{N} \frac{F_i \cdot F_j}{r_{ij}} + \frac{k}{\sqrt{2}} (\mathbf{D}^2)^{1/2} , \tag{3.1}$$

where

$$\mathbf{D} = \sum_{i=1}^{N} F_i \mathbf{r}_i$$

is the color-dipole-moment operator. The string tension k is determined by the bag constant B and α_s via

$$k = \left[\frac{32\pi}{3} \alpha_s B \right]^{1/2} . \tag{3.2}$$

The subscript S on the potential indicates that it is expected to be valid at small distances. Note that as a result of the square-root operation in Eq.(3.1) the confining term is indeed a many-body potential.

It is the fact that Eq. (3.1) applies to any number N of quarks and/or antiquarks that enables us to calculate the energy of individual mesons and dimesons on the same footing.[6] For the two-body system, the potential becomes

$$V_S^{(2)} = -\frac{4}{3} \frac{\alpha_s}{r} + (\tfrac{2}{3})^{1/2} kr \tag{3.3}$$

which shows that the effective string tension at small distances is only ~ 0.8 of its value at very large distances where the bag becomes a tube of flux.[7,9]

Even though the dimesons we shall be discussing are smaller than 1 fm, a portion of the wave function extends farther out, so to be quantitative it is necessary to also consider the behavior of the potential at larger distances. The portion of configuration space that is most important for this purpose consists of one $(Q\bar{q})$ pair separating from the other. In this region the bag becomes deformed and must even be capable of undergoing fission. This is a difficult technical problem that we have not yet solved, so we do not know the correct form of the potential at intermediate distances. What we shall do instead is to use some physical arguments to write down the potential matrix at large distances, and then use a simple parametrization to make a smooth transition.[10]

The natural color basis for discussing this transition is the one in which the separating $(Q\bar{q})$ pairs are either both in color singlets or both in color octets coupled to an overall singlet. Labeling the two quarks as 1 and 3, and the two antiquarks as 2 and 4, and calling $R_{12,34}$ the distance between the midpoints of the two pairs, the color basis for this geometry is chosen to be

$$\begin{aligned} \psi_1 &= |\,[(12)^1(34)^1]^1\rangle , \\ \psi_8 &= |\,[(12)^8(34)^8]^1\rangle . \end{aligned} \tag{3.4}$$

For $R_{12,34} \gtrsim 1$ fm we expect the potential to become

$$V_L^{(4)}(12,34)=\begin{bmatrix} V_S^{(2)}(r_{12})+V_S^{(2)}(r_{34}) & O \\ O & fk_8R_{12,34} \end{bmatrix} . \quad (3.5)$$

The significance of the various matrix elements is as follows. The diagonal element in the singlet-singlet state is the sum of the two potential energies *within* the individual $(Q\bar{q})$ pairs, with no interaction between them. The diagonal element in the octet-octet state is the confining part of the bag-model potential energy between two octets. Referring to Eq. (3.2) shows that $k\sim(F^2)^{1/2}$, and consequently

$$\frac{k_8}{k}=\left[\frac{F_8\cdot F_8}{F_3\cdot F_{\bar{3}}}\right]^{1/2}=\left[\frac{3}{4/3}\right]^{1/2}=\frac{3}{2} . \quad (3.6)$$

The factor f has the value $(\frac{2}{3})^{1/2}$ at small values of the separation of the two octets, where a spherical bag is valid, and becomes unity at large separations, where a tube of flux develops.

Concerning the off-diagonal element O, it must fall off sufficiently rapidly with distance so that there are no van der Waals forces, and this means at least exponentially. Not knowing the correct strength for this term we simply set $O=0$. As our method of combining V_S and V_L (see below) involves a Gaussian weight factor, the full potential V does have an off-diagonal element with Gaussian falloff at large distance.

Since the potential energy depends only on the positions and color charges of the sources, it must be symmetric under the interchange of all coordinates of the two quarks or the two antiquarks; hence we also need a second quantity $V_L(14,23)$ obtained by interchanging $2\leftrightarrow 4$ in Eqs. (3.4) *and* (3.5). [Note that Eq. (3.1) already possesses this symmetry.] We now combine the small- and large-distance components of the potential smoothly by taking

$$\begin{aligned} V^{(4)}=&V_S^{(4)}[1-W(12,34)-W(14,23)] \\ &+V_L^{(4)}(12,34)W(12,34) \\ &+V_L^{(4)}(14,23)W(14,23) , \end{aligned} \quad (3.7)$$

where

$$\begin{aligned} W(ij,kl)=&\Theta(\beta R_{ij,kl}^2-r_{ij}^2-r_{kl}^2) \\ &\times[1-\exp(-R_{ij,kl}^2/d^2)] . \end{aligned} \quad (3.8)$$

The Θ function is defined to be 1 if its argument is positive and zero otherwise, and $\beta\leq 2$ guarantees that the two Θ functions occurring in Eq. (3.7) are mutually exclusive, i.e., at most one of them can be nonvanishing in any given geometry. The parameter d in Eq. (3.8) determines (along with β) the relative amounts of the small- and large-distance portions of the potential, and according to the discussion above we choose $d=1$ fm but also show some results with $d=0.5$ fm and $d=\infty$.

Since light quarks ($m\sim 0.3$ GeV) are quite relativistic under the influence of this potential, we use the "semirelativistic" (SR) operator $(\mathbf{p}^2+m^2)^{1/2}$ for the kinetic energy:

$$E_K=\sum_i\sqrt{p_i^2+m_i^2} \ \ (\text{SR}) . \quad (3.9)$$

For some cases we also report results with the nonrelativistic (NR) expression:

$$E_K=\sum_i(p_i^2/2m_i+m_i) \ \ (\text{NR}) . \quad (3.10)$$

The interaction parameters and masses used in this study are given in Table I below. In addition to the spin-independent potential given by Eqs. (3.3) and (3.7) we also include, as a perturbation, the hyperfine interaction. The details are presented in the Appendix.

IV. CALCULATIONS

In order to determine the binding energies of the dimesons, it is necessary to calculate the ground-state energy of both the mesons and dimesons. Accurate variational methods have been used to determine the ground state of the $Q\bar{q}$ systems. By diagonalizing the Hamiltonian within a suitable subspace, the energy is easily determined within ~ 1 MeV. For the dimesons, we have used the Green's-function Monte Carlo (GFMC) method to project out the ground-state energy. The GFMC method is exact in principle, yielding ground-state energies subject to only a statistical error.

The Schrödinger equation may be solved numerically for the meson's ground state when a nonrelativistic kinetic energy expression is used. The semirelativistic kinetic energy operator is nonlocal, however, involving all powers of the momentum. Therefore, we use variational methods to solve for the ground state.

We take the trial wave function for the meson to be a sum of Gaussians:

$$\psi=\sum_i c_i\exp[-(r_{Q\bar{q}}/b_i)^2] . \quad (4.1)$$

The ranges b_i of the Gaussians are variational parameters, and their relative strengths are determined by first obtaining an orthonormal basis from the set of Gaussians and then diagonalizing the Hamiltonian matrix in this basis. A Gaussian form is chosen to simplify the evaluation of the matrix elements. The kinetic energy matrix elements are evaluated in momentum space, and the potential-energy terms in coordinate space.

The method has been tested by varying the range and number of Gaussians. Typically, 7–10 Gaussians are used, and this seems to provide a ground-state energy accurate to approximately 1 MeV. For comparison, we have also calculated the meson's ground state using a simple one-parameter wave function:

$$\psi=\exp(-\alpha r_{Q\bar{q}}) . \quad (4.2)$$

In the semirelativistic case, this trial function gives an energy only slightly (5–10 MeV) higher than the sum of Gaussians, while in the nonrelativistic case the energy is within 1–3 MeV of the exact result. The two types of wave functions are compared in Fig. 1. The principal difference appears to occur in their small-r behavior. The semirelativistic kinetic energy operator produces a

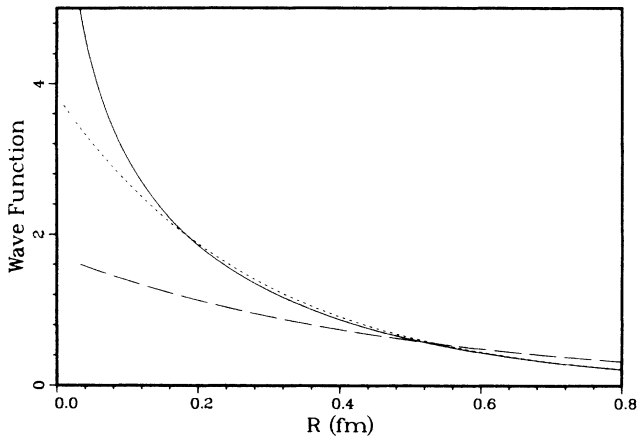

FIG. 1. The ground-state wave function of the $b\bar{u}$ meson. The solid curve is obtained from a sum of Gaussians [Eq. (4.1)], while the dotted line is a single exponential. The dashed line is the nonrelativistic wave function.

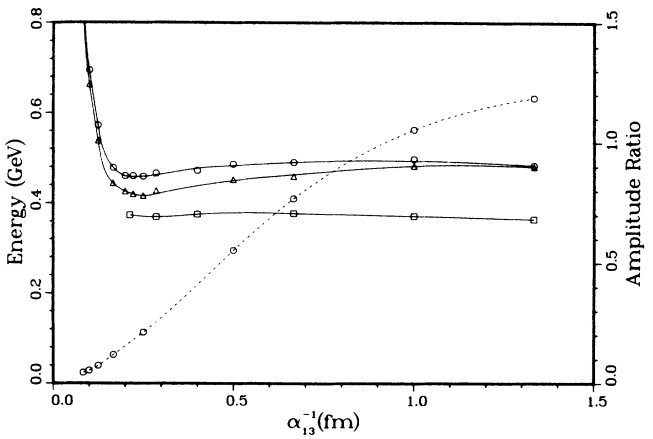

FIG. 2. Variational calculations of the minimum energy of the $bb\bar{u}\bar{d}$ system as a function of the meson separation parameter α_{13}^{-1}. The energies are plotted as solid curves for three choices of the cutoff parameter d (squares correspond to $d=\infty$, triangles to 1.0 fm, and circles to 0.5 fm). The size of the symbols corresponds to the statistical error of the Monte Carlo calculations. The dashed line gives the magnitude of the ratio of the amplitude in the $6\bar{6}$ channel to that in the $\bar{3}3$ channel for $d=0.5$ fm (right-hand scale). Two isolated mesons correspond to a ratio of $\sqrt{2}$. Parameter set $C1$ was used in these calculations, and the dotted line represents the sum of the energies of $(b\bar{u})$ and $(b\bar{d})$.

divergent wave function (although not probability) as $r\to 0$, and the one-parameter exponential wave function cannot reproduce this behavior. The nonrelativistic wave function is also shown. As is apparent in the figure, the semirelativistic Hamiltonian gives a significantly smaller radius.

The calculations of the ground-state properties of the dimesons are more difficult. Standard variational Monte Carlo methods[11] are first used to determine an upper bound to the true ground-state energy. The Metropolis method is employed, and both channels are summed at each point in the walk.

The variational wave function of the dimesons is taken to be

$$\psi=[\exp(-\alpha_c r_{12}-\alpha_c r_{34}-\alpha_{13} r_{13})+(1\leftrightarrow 3)]\psi_3 + c_m[\exp(-\alpha_c r_{12}-\alpha_c r_{34}-\alpha_{13} r_{13})-(1\leftrightarrow 3)]\psi_6 , \tag{4.3}$$

where ψ_3 (ψ_6) indicates a coupling of a $\bar{3}$ and 3 (6 and $\bar{6}$) to a total color singlet. The variational parameters are α_c, α_{13}, and c_m. This wave function accurately represents the system in the limit of two separated mesons. For the case $\alpha_{13}=0$, we obtain an antisymmetrized product of two meson wave functions, each of which is represented by an exponential in the pair separation. The parameter c_m will give a probability for the $6\bar{6}$ channel that is twice that of the $\bar{3}3$ channel in this case.

As the quark mass increases, the parameter α_{13} becomes large, and the wave function of Eq. (4.3) will describe independent orbits of the light quarks around the heavy quarks. In this limit, the parameter c_m will be very small, since there is a Coulomb repulsion between the heavy quarks in the $6\bar{6}$ channel. Results of variational calculations of the $bb\bar{u}\bar{d}$ meson are shown in Fig. 2, which illustrates the transition from a bound dimeson to two isolated mesons. The minimum variational energy is plotted as function of the heavy-quark separation parameter $(1/\alpha_{13})$ for several choices of the cutoff parameter d. Interaction parameter set $C1$ (see Table I) was used in each case, along with a slightly modified form of the cutoff.

The variational energy passes through a minimum as the two heavy quarks are separated. For larger separations (and a finite cutoff d), the energy will increase to the variational energy of two isolated mesons, each parametrized by an exponential in the internal coordinate. The relative amplitudes of the $\bar{3}3$ and $6\bar{6}$ states are also plotted in Fig. 2. For small separations, the amplitude in the $6\bar{6}$ channel is very small due to the Coulomb repulsion. The magnitude of the amplitude in the $6\bar{6}$ channel gradually increases, approaching $\sqrt{2}$ times that of the $\bar{3}3$ channel for large separations, which is the correct ratio for two isolated mesons.

Results for the $tt\bar{u}\bar{d}$ dimeson are shown in Fig. 3. In this case the α_s associated with the tt color Coulomb attraction has been reduced to 0.32 to take into account the effects of asymptotic freedom. For this heavy-quark mass, the dimeson is deeply (~ 700 MeV) bound, and the minimum variational energy is obtained with a tightly bound QQ pair ($\alpha_{13}^{-1}\approx 0.03$ fm).

The variational parameters for a variety of dimeson systems are given in Table III below. The effects of the semirelativistic kinetic energy expression are seen in a comparison of the values of α_c obtained for the $bb\bar{u}\bar{d}$ dimeson with parameter sets B and C. The semirelativistic interaction (B) produces a smaller overall size for the wave function of the light quarks.

The major deficiency of this variational wave function appears to be the fact that there is no correlation between the two light quarks. In the nonrelativistic case, this correlation can be trivially included and the varia-

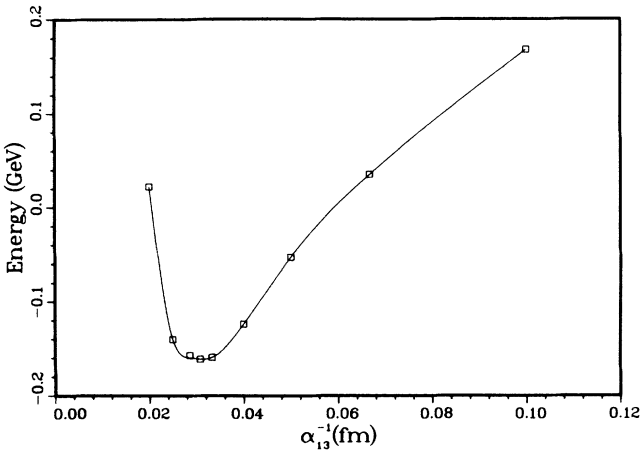

FIG. 3. The variational energy of the $tt\bar{u}\bar{d}$ dimeson vs the separation parameter α_{13}^{-1}. The energy of two isolated $t\bar{u}$ mesons is 0.45 GeV on this scale.

tional ground-state energy reduced. For a semirelativistic kinetic energy, this additional correlation greatly increases the difficulty of Fourier transforming the wave function and calculating the kinetic energy. Therefore, we rely upon the Green's-function Monte Carlo method to introduce these correlations.

The variational energy of these wave functions is larger than that of two separated mesons in some cases, and therefore could in principle be reduced by setting α_{13} to zero. However, we use the Green's-function Monte Carlo method to determine the true ground state, which has a very small overlap with the wave function of two separated mesons.

Green's-function Monte Carlo[12–16] methods are very attractive for this study because we are primarily interested in the ground-state properties of the system. Two difficulties are immediately apparent, however, in applying standard methods to the dimeson system. The semirelativistic kinetic energy operator necessitates the use of a different Green's function. We employ the short-time approximation in these calculations, where the full Green's function $\langle \mathbf{R}' \mid \exp(-H\Delta\tau) \mid \mathbf{R} \rangle$ is approximated by the product of a free particle Green's function $G(\mathbf{R},\mathbf{R}',\Delta\tau)$ and $\exp(-V\Delta\tau)$. The nonrelativistic Green's function is

$$G(\mathbf{R},\mathbf{R}',\Delta\tau)=\left[\frac{1}{4\left[\frac{\hbar^2}{2m}\right]\Delta\tau\pi}\right]^{3/2}\exp(-mc^2\Delta\tau)\times\exp\left[-\frac{(\Delta R)^2}{4\left[\frac{\hbar^2}{2m}\right]\Delta\tau}\right], \tag{4.4}$$

with

$$\Delta R=|\mathbf{R}-\mathbf{R}'| \ . \tag{4.5}$$

For the semirelativistic kinetic energy operator, the Green's function is

$$G(\mathbf{R},\mathbf{R}',\Delta\tau)=\frac{4\pi}{(2\pi)^3}\frac{\beta\alpha^2}{\Delta R^3(1+\beta^2)}K_2[\alpha(1+\beta^2)^{1/2}] \ , \tag{4.6}$$

where

$$\beta=\frac{\hbar c\Delta\tau}{\Delta R} \ , \tag{4.7}$$

$$\alpha=mc\Delta R/\hbar \ , \tag{4.8}$$

and K_2 is a Bessel function of order 2.

This Green's function differs from the Gaussian primarily in that there is a long-range part whose range is equal to the inverse of the mass and independent of the time step. The magnitude of this long-range part is proportional to the time step, however, so that the Monte Carlo root-mean-square step size is the same as in the nonrelativistic case. In the limit of large $m\Delta\tau$ and small $\Delta R/(\hbar c\Delta\tau)$, the two Green's functions become identical. The nonrelativistic and semirelativistic Green's functions are compared in Fig. 4.

The other difficulty in treating these systems is that there are two coupled channels (the $\bar{3}3$ and $6\bar{6}$ color states). A straightforward extension[14] of standard[15,16] methods is sufficient to treat these systems. The exponential of the potential is evaluated by diagonalizing the interaction at each step in the walk. The standard difficulties associated with fermion systems[16] are largely absent in these calculations. Since we are searching for the lowest-energy state of any spatial symmetry, the random walks converge to the physical ground state. Although negative weights do eventually appear due to the spatial antisymmetry in the $6\bar{6}$ channel, the increase in noise is very slow. Consequently, the ground-state energy may be easily determined before large statistical errors are introduced.

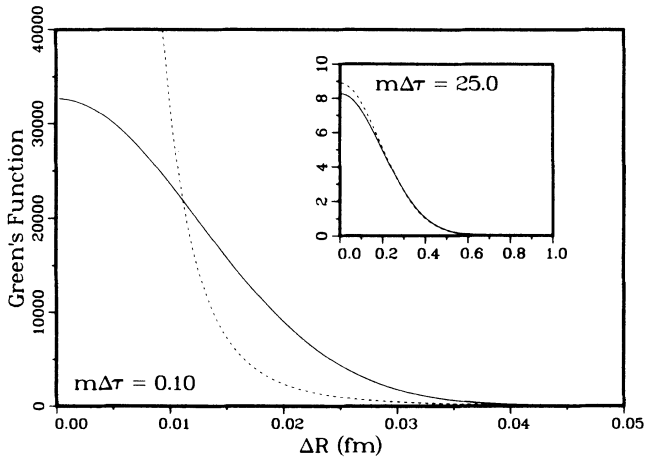

FIG. 4. A comparison of the nonrelativistic (solid lines) and semirelativistic (dashed lines) Green's functions for two values of $m\Delta\tau$. The mass is 5 GeV in both cases. The product $m\Delta\tau=25$ is much too large for this system, but is shown to illustrate the correspondence of the two Green's functions for large times.

V. RESULTS

The results of our calculations are summarized in Tables I–VI. We first discuss the results for the mesons, and then the binding energy of the dimesons with and without the hyperfine interaction.

Several sets of interaction parameters[6,8] have been used in these studies so that the model dependence of the results can be determined. The various choices of parameters are given in Table I. Set A provides a good fit to $(b\bar{b})$ and $(c\bar{c})$ spectra; sets B and C only fit $(b\bar{b})$. The labels of the different parameter sets are chosen so that all sets labeled by the same letter produce the same meson ground state. Different numbers indicate different interactions in the transition region, which only affects the dimesons. Table II gives the ground-state energies of various mesons with different parameter sets. Results are given for the spin-independent interaction. The change in energy of the $S=0$ state due to the hyperfine interaction is given in the last column. As indicated in Table II, the spin average of the light-heavy experimental meson energies do not agree well with the calculated values. (For the $b\bar{b}$ meson, we have assumed an experimental hyperfine splitting of 80 MeV, since the energy of the η_b is not known.) The agreement with experimental meson masses could be improved somewhat by reducing the light-quark mass, as shown in Fig. 5. The discrepancy cannot be entirely eliminated in this manner, however. We proceed with the expectation that the errors will largely cancel when calculating the difference in energy of a dimeson and two mesons. In addition, we have performed calculations with two very different sets of interaction parameters.

A. No hyperfine interaction

Results for the dimesons are presented in Tables III–V. Table III gives the variational parameters that were used for the GFMC calculations of the dimesons. These parameters were not carefully optimized for every case, since GFMC converges to the ground state for any trial wave function that is not orthogonal to that state. In particular, the dimeson wave functions were not changed for different cutoffs of the four-quark interaction in Eq. (3.8).

Tables IV and V present the ground-state energies of the various dimesons, omitting the hyperfine interaction (in both mesons and dimesons). The $(bb\bar{u}\bar{d})$ dimeson has nearly the same binding as the $(bc\bar{u}\bar{d})$ and $(cc\bar{u}\bar{d})$ systems, as seen in Table V. The b quark is not heavy

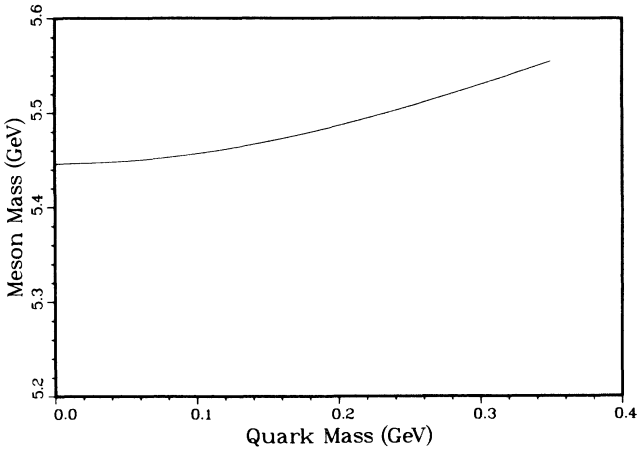

FIG. 5. Energy of the $c\bar{u}$ meson as a function of the light-quark mass (interaction parameter set A).

enough for the bb Coulomb attraction to completely dominate [Eqs. (2.3)–(2.5)] the other energies in the problem.

Table IV shows that the $6\bar{6}$ channel has the smallest probability for the $bb\bar{u}\bar{d}$ dimeson, as expected from the arguments given in Sec. II. Even for this case, however, the $6\bar{6}$ channel is significant. The semirelativistic kinetic energy operator allows the wave function of the light quarks to be restricted to a fairly small region, so that the separation between the heavy quarks is not negligible compared to typical light-heavy quark separations.

Prior to the introduction of hyperfine perturbations, the $bb\bar{u}\bar{d}$ dimeson is bound by approximately 90 MeV. This result does not depend strongly upon the choice of interaction in the transition region [Eq. (3.5)]. Parameter set $B1$ yields a smaller binding energy, approximately 40 MeV. The spin-independent interaction also results in bound $bc\bar{u}\bar{d}$ and $cc\bar{u}\bar{d}$ dimesons, with only a slight decrease in binding energy as the mass of the heavy quark decreases. The most obvious change in the system as the heavy-quark mass decreases is the increase in magnitude of the $6\bar{6}$ component of the wave function, as indicated in Table IV. For two isolated mesons, the probability of the $6\bar{6}$ component would be twice that of the $\bar{3}3$ component.

There is a greater uncertainty in the $cc\bar{u}\bar{d}$ dimeson arising from uncertainties in the interaction. As described in Sec. III, the potential energy as the dimeson separates into two mesons in not well determined by the dipole approximation to the bag [Eq. (3.5)]. Therefore,

TABLE I. Interaction parameters used for the dimeson calculations. All energies and masses are given in GeV and all distances in Fermi. The column kinetic energy (KE) tells whether the nonrelativistic (NR) or semirelativistic (SR) kinetic energy expression is used. Interaction set $A3$ is the same as $A1$ except that the Gaussian cutoff [Eq. (3.8)] is squared, producing a sharper cutoff. The final two columns are the parameters in that equation.

Parameter set	α_s	$B^{1/4}$	KE	m_u, m_d	m_c	m_b	m_t	d	β
$A1, A3$	0.370	0.245	SR	0.35	1.364	4.781	60.0	1.0	2.0
$A2$	0.370	0.245	SR	0.35	1.364	4.781	60.0	1.0	0.5
$B1$	0.495	0.145	SR	0.35	1.685	4.970	60.0	1.0	2.0
$C1$	0.495	0.145	NR	0.35	1.685	4.970	60.0	1.0	2.0

TABLE II. Ground-state properties of various mesons. The third column gives the variational parameter α [Eq. (4.2)]. The ground-state energies are obtained with the parametrization given in Eq. (4.1). The calculated and experimental masses are spin averages of the $S=0$ and $S=1$ state, and the last column gives the change in energy of the $S=0$ state due to the hyperfine interaction. All energies and masses are in GeV.

Parameter set	Quark content	Variational parameter α (fm^{-1})	E (without hyperfine)	m_{calc}	m_{expt}	ΔE (hyperfine)
$A1$	$c\bar{u}$	3.3	0.535	2.25	1.97	−0.111
	$b\bar{u}$	4.0	0.427	5.56	5.31	−0.044
	$c\bar{c}$	4.1	0.318	3.05	3.07	−0.076
	$b\bar{b}$	8.4	−0.135	9.43	9.44	−0.020
$B1$	$c\bar{u}$	2.9	0.162	2.20	1.97	−0.103
	$b\bar{u}$	3.6	0.088	5.41	5.31	−0.053
	$c\bar{c}$	4.4	−0.070	3.30	3.07	−0.085
	$b\bar{b}$	10.4	−0.552	9.39	9.44	−0.032
$C1$	$b\bar{u}$	2.2	0.229	5.55	5.31	
	$b\bar{b}$	8.8	−0.478	9.46	9.44	
	$t\bar{u}$	2.2	0.226	60.58		

our results depend to some extent on what parametrization is chosen for the interaction in this region, as shown in Table IV. The $cc\bar{u}\bar{d}$ meson is larger than the $bb\bar{u}\bar{d}$ and consequently more sensitive to the interaction in this region.

B. With hyperfine interaction

We now examine the effect of including the hyperfine interaction according to the prescription given in the Appendix. The ground state of each meson is split into a pair of levels with the $S=1$ state shifted upward by $\frac{1}{3}$ the amount the $S=0$ states moves downward. The latter numbers are given in Table II.

The hyperfine shift in the dimesons is shown in Table VI for each spin assignment. There does not appear to be a simple argument to determine which spin state is lowest in energy. The factor $(m_i m_j)^{-1}$ in Eq. (A1) tends to make the light-light pair dominate over the light-heavy pairs; but the spatial matrix elements are smaller for the former, and there are four of the latter. It turns out that in the $(bb\bar{q}\,\bar{q}')$ system the lowest-energy state has the spin assignment $(S24,S13,S)=(0,1,1)$ where $S13$ is the spin of the two heavy particles, $S24$ is the spin of the two light particles, and S is the total spin. Since the space-color wave function is antisymmetric under the interchange of $\bar{q}$ and $\bar{q}'$ [see Eq. (4.3)], the $S24=0$ state is available only to an isoscalar pair. For the $(bc\bar{q}\,\bar{q}')$ and $(cc\bar{q}\,\bar{q}')$ systems, on the other hand, the lowest state has $S24=1$, which must be an isovector.

The hyperfine levels are also shown in Figs. 6–8. Examination of Fig. 6 shows that each level of $(bb\bar{q}\,\bar{q}')$ is lower in energy than the threshold for two mesons $(b\bar{q})+(b\bar{q}')$ with the same total spin. The ground state (0,1,1) of the dimeson, being 70 MeV below the BB threshold, is stable against all strong and electromagnetic decays. The (1,1,0) state can only decay electromagnetically and will therefore be a sharp resonance. The same is true of the (1,1,1) state, which is very close to the BB threshold but cannot decay strongly because of parity. The (1,1,2) state can decay strongly to BB but the angular momentum barrier will probably keep it narrow.

Figure 7 shows the corresponding level diagram for the $(cc\bar{q}\,\bar{q}')$ dimeson. Here the ground state (1,1,0) is 60 MeV above the DD threshold and can only be a broad

TABLE III. Variational parameters used for the dimeson calculations. The form of the wave function is given in Eq. (4.3).

Parameter set	Quark content	α_{13} (fm^{-1})	α_c (fm^{-1})	c_m
A	$bb\bar{u}\bar{d}$	4.5	3.0	1.4
	$bc\bar{u}\bar{d}$	3.0	3.0	1.4
	$cc\bar{u}\bar{d}$	2.5	3.0	1.4
B	$bb\bar{u}\bar{d}$	4.5	3.0	1.1
C	$bb\bar{u}\bar{d}$	4.0	2.0	0.6
	$tt\bar{u}\bar{d}$	32.5	2.0	0.3

TABLE IV. A comparison of results for the $bb\bar{u}\bar{d}$ and $cc\bar{u}\bar{d}$ with different potential cutoffs [Eqs. (3.7) and (3.8)]. The third column gives the relative probability of the $\mathbf{6\bar{6}}$ channel, defined such that $\langle\psi_{6\bar{6}}|\psi_{6\bar{6}}\rangle+\langle\psi_{\bar{3}3}|\psi_{\bar{3}3}\rangle=1$. No hyperfine interactions are included.

Quark content	Parameter set	$\langle\psi_{6\bar{6}}\|\psi_{6\bar{6}}\rangle$	Energy (GeV)
$bb\bar{u}\bar{d}$	$A1$	0.23±0.01	0.765±0.004
	$A2$	0.26±0.01	0.756±0.003
	$A3$	0.23±0.02	0.773±0.008
$cc\bar{u}\bar{d}$	$A1$	0.33±0.01	0.995±0.007
	$A2$	0.41±0.01	0.955±0.005

TABLE V. The ground-state energies of the dimesons, and their binding energies with respect to two separated mesons. The hyperfine interaction is not included in either the dimesons or mesons. All energies are in GeV. The statistical errors in the Monte Carlo calculations are approximately 10 MeV in all cases.

Parameter set	Quark content	E	Binding energy
$A1$	$bb\bar{u}\bar{d}$	0.765	0.09
	$bc\bar{u}\bar{d}$	0.875	0.09
	$cc\bar{u}\bar{d}$	0.955	0.08

resonance. The (0,1,1) and (1,1,1) states, on the other hand, can only decay electromagnetically. The energies of this system, and also the mixed dimeson ($bc\bar{q}\,\bar{q}'$), are more uncertain, however, since they depend more sensitively on the model parameters.

The level diagram for ($bc\bar{q}\,\bar{q}'$) is shown in Fig. 8. The ground state (1,1,0) is degenerate with the BD threshold within the numerical accuracy of the calculations. The (0,1,1) state and the lower mixture of (1,0,1) and (1,1,1) are about 20 MeV above the BD threshold, and will decay electromagnetically.

VI. SUMMARY

For sufficiently large quark mass m (and fixed antiquark mass $\bar{m}$), the dimeson ($Q^2\bar{q}^2$) *must* be stable against strong decay. The color Coulomb attraction of the two quarks in the color $\bar{3}$ state dominates all the other energies in the problem.

We have employed a confining interaction derived from a Born-Oppenheimer approximation to the MIT bag model in order to estimate the binding energies of various dimesons. Generalizations of Green's-function Monte Carlo methods have been introduced to allow us to treat the semirelativistic and coupled channel (see also Ref. 14) aspects of the dimeson systems. These methods should prove very valuable in many quark model applications.

We find that the 1^+ isoscalar dimeson $T(bb\bar{u}\bar{d})$ (Ref. 17) is bound by ~ 70 MeV in this model, with only a

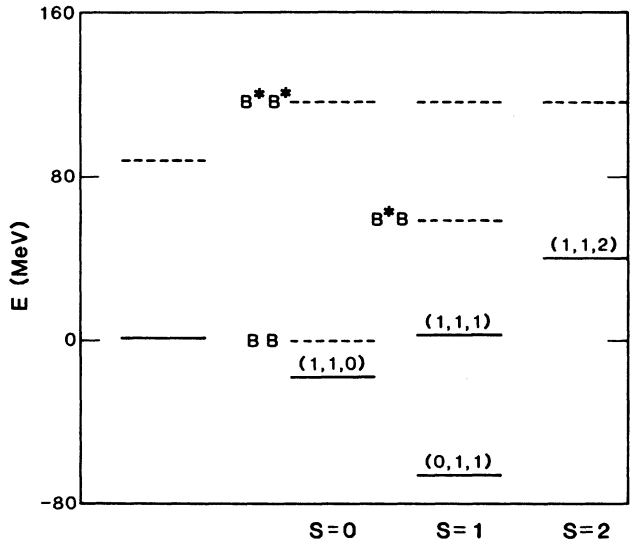

FIG. 6. Hyperfine structure of the $bb\bar{q}\,\bar{q}'$ system. States of two mesons are indicated by dashed lines and dimesons are shown as solid lines labeled by ($S_{\bar{q}\bar{q}'}$,S_{bb},S) where S is the total spin. The levels on the left omit the hyperfine interaction.

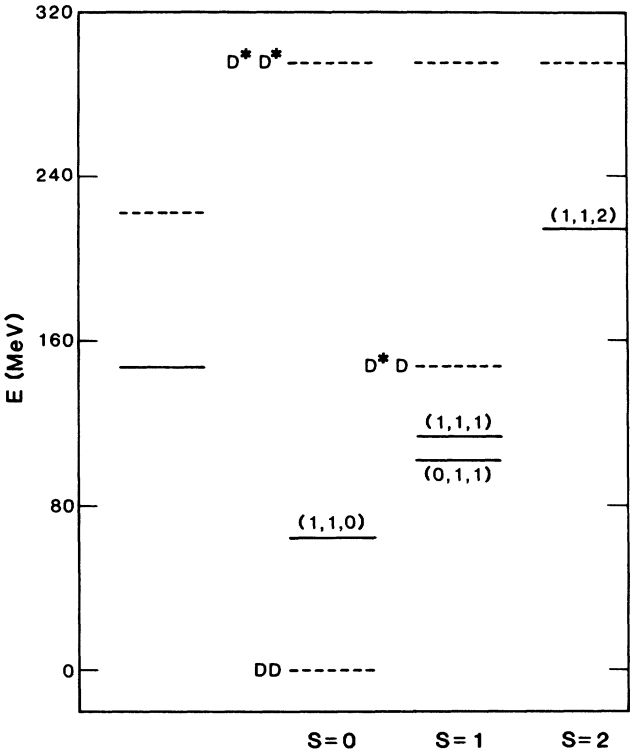

FIG. 7. Hyperfine structure of the $cc\bar{q}\,\bar{q}'$ system. See caption to Fig. 6.

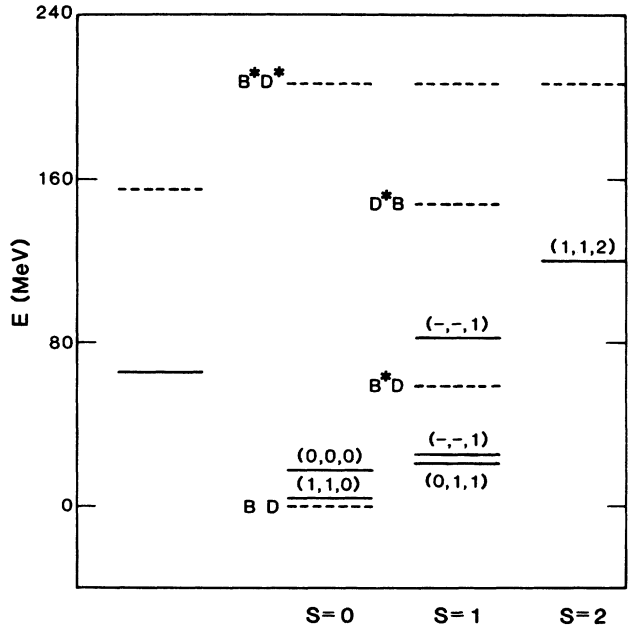

FIG. 8. Hyperfine structure of the $bc\bar{q}\,\bar{q}'$ system. See caption to Fig. 6. The dimeson levels labeled $(-,-,1)$ are mixtures of the (1,0,1) and (1,1,1) states.

TABLE VI. A comparison of the energy of the dimeson states with that of two isolated mesons. The dimeson states are labeled by (S_{24},S_{13},S), where S_{24} is the combined spin of the light antiquarks, S_{13} is the spin of the pair of heavy quarks, and S is the total spin. The third column lists the change in energy due to the hyperfine interaction. The fourth column gives the difference between the energy of the dimeson and the lowest-energy state of two mesons (pseudoscalar), and the last column shows the difference between the dimeson and the lowest state of two mesons with the same spin (see text). All energies are in GeV.

Quark content	(S_{24},S_{13},S)	ΔE_H	$E-E_0$ (two mesons)	$E-E_S$ (two mesons)
$bb\bar{u}\bar{d}$	(1,1,0)	−0.020	−0.02	−0.02
	(0,1,1)	−0.065	−0.07	−0.13
	(1,1,1)	0.005	0.00	−0.06
	(1,1,2)	0.040	0.04	−0.08
$bc\bar{u}\bar{d}$	(1,1,0)	−0.060	0.00	0.00
	(0,0,0)	−0.050	0.02	0.02
	(0,1,1)	−0.045	0.02	−0.04
	0.84(1,1,1)−0.54(1,0,1)	−0.040	0.03	−0.03
	0.54(1,1,1) + 0.84(1,0,1)	0.015	0.08	0.02
	(1,1,2)	0.055	0.12	−0.09
$cc\bar{u}\bar{d}$	(1,1,0)	−0.080	0.07	0.07
	(0,1,1)	−0.045	0.10	−0.05
	(1,1,1)	−0.035	0.11	−0.03
	(1,1,2)	0.070	0.22	−0.08

small dependence on the interaction in the transition region (the dimeson separating into two mesons). This particle can only decay weakly. The $(cc\bar{u}\bar{d})$ dimeson is not bound, while the $(bc\bar{u}\bar{d})$ dimeson is a borderline case, but these results are more uncertain. In addition, there are $S=1$ states in all systems that can only decay electromagnetically. The calculations with the b quark indicate that its mass is not large enough for the Coulomb attraction in the $\bar{3}$ state to completely dominate.

The ground-state energy obtained with Green's-function Monte Carlo methods is significantly lower than the variational upper bounds obtained with the trial wave function, Eq. (4.3). For example, the GFMC ground-state energy is approximately 50 MeV below the variational reuslts of Fig. 2, for the same Hamiltonian. With the semirelativistic Hamiltonians, the decrease in energy is even larger, typically around 100 MeV.

ACKNOWLEDGMENTS

L.H. wants to thank H. Lipkin for helpful discussions about the hyperfine interaction. We thank N. Metropolis for his proposal to designate four-quark systems with the letter T (Ref. 17). This research was supported by the U.S. Department of Energy.

TABLE VII. The color matrix elements used in these calculations. $F_i\cdot F_j=F_k\cdot F_l$ for distinct values of i, j, k, and l.

Pairs	$\langle\bar{3}3\mid F_i\cdot F_j\mid\bar{3}3\rangle$	$\langle\bar{3}3\mid F_i\cdot F_j\mid 6\bar{6}\rangle$	$\langle 6\bar{6}\mid F_i\cdot F_j\mid 6\bar{6}\rangle$
13,24	$-\frac{2}{3}$	0	$\frac{1}{3}$
12,34	$-\frac{1}{3}$	$1/\sqrt{2}$	$-\frac{5}{6}$
14,23	$-\frac{1}{3}$	$-1/\sqrt{2}$	$-\frac{5}{6}$

APPENDIX: HYPERFINE INTERACTION

The effect of the hyperfine interaction has been included in first-order perturbation theory in our calculations. Typically, this interaction is written as[18]

$$V_H=-\frac{2\pi}{3}\alpha_s\sum_{i<j}F_i\cdot F_j\sigma_i\cdot\sigma_j\frac{\delta^3(\mathbf{r}_{ij})}{m_i m_j}\ . \tag{A1}$$

The delta function in quark separation cannot be used with the semirelativistic kinetic energy operator, however, since the wave functions diverge at zero separation. By introducing a form factor at each quark-gluon vertex, one can make the replacement

$$\delta^3(\mathbf{r}_{ij})\rightarrow N\exp(-r_{ij}^2/d^2)\ , \tag{A2}$$

where the normalization N is such that the volume integral of the interaction is unchanged. Previous studies of mesons and baryons[19] have indicated that the width of the Gaussian necessary to fit the experimental hyperfine splitting changes with quark mass. This change is presumably associated with the Compton

TABLE VIII. The spin matrix elements used to compute the hyperfine interaction (see the Appendix). The matrix elements of the other pairs may be obtained from $\langle\sigma_1\cdot\sigma_2\rangle$ by symmetry arguments.

State (S_{13},S_{24},S)	$\langle\sigma_1\cdot\sigma_3\rangle$	$\langle\sigma_2\cdot\sigma_4\rangle$	$\langle\sigma_1\cdot\sigma_2\rangle$
$\langle 000\mid\sigma_i\cdot\sigma_j\mid 000\rangle$	−3	−3	0
$\langle 110\mid\sigma_i\cdot\sigma_j\mid 110\rangle$	1	1	−2
$\langle 111\mid\sigma_i\cdot\sigma_j\mid 111\rangle$	1	1	−1
$\langle 112\mid\sigma_i\cdot\sigma_j\mid 112\rangle$	1	1	1
$\langle 011\mid\sigma_i\cdot\sigma_j\mid 011\rangle$	−3	1	0
$\langle 101\mid\sigma_i\cdot\sigma_j\mid 101\rangle$	1	−3	0
$\langle 101\mid\sigma_i\cdot\sigma_j\mid 111\rangle$	0	0	$\sqrt{2}$

wavelength of the quark.

We have adopted a similar attitude in this work, adjusting the range of the interaction to give a rough fit to the meson splittings. For pairs consisting of one light and one heavy quark, we use a range of 0.25 fm, while for pairs of heavy (c or b) quarks we use $d=0.15$ fm. The resulting meson hyperfine splittings are given in Table II.

It might be expected from Ref. 19 that the range associated with two bottom quarks should be significantly smaller. We have experimented with a shorter-range (0.07-fm) interaction for the $bb\bar{u}\bar{d}$ dimesons. This change produced only a very small change in energy, approximately 1–2 MeV.

There are only two possible spin states for the spatial ground state of the meson. The expectation value of the hyperfine interaction can be easily calculated from Eq. (A1). The situation is somewhat more complicated for the dimesons, however.

There are many possible spin states of the dimeson system. We have chosen to use the basis where the spin of the two light quarks are coupled to a definite spin S_{24}, the two heavy quarks are coupled to a spin S_{13}, and finally these two spins are coupled to a total spin S. The color and spin matrix elements used in our calculations are given in Tables VII and VIII.

It is important to remember that not all of these spin states are physical (antisymmetric) in every four-quark system. For example, two identical quarks in a combined space-color-symmetric state must be in an antisymmetric spin state. For this reason, a dimeson system such as $bb\bar{u}\bar{d}$ has more possible states than $bb\bar{u}\bar{u}$. Of course, still more states are accessible to a $bc\bar{u}\bar{d}$ dimeson.

[1]J. P. Ader, J. M. Richard, and P. Taxil, Phys. Rev. D **25**, 2370 (1982).
[2]J. L. Ballot and J. M. Richard, Phys. Lett. **123B**, 449 (1983).
[3]L. Heller, in *Workshop on Nuclear Chromodynamics, Quarks, and Gluons in Particle and Nuclei,* edited by S. Brodsky and E. Moniz (World Scientific, Singapore, 1986), p. 306.
[4]C. Zouzou *et al.*, Z. Phys. C **30**, 457 (1986).
[5]H. J. Lipkin, Phys. Lett. B **172**, 242 (1986).
[6]L. Heller and J. A. Tjon, Phys. Rev. D **35**, 969 (1987).
[7]A. T. Aerts and L. Heller, Phys. Rev. D **23**, 185 (1981); **25**, 1365 (1982).
[8]L. Heller and J. A. Tjon, Phys. Rev. D **32**, 755 (1985).
[9]K. Johnson, in *Current Trends in the Theory of Fields,* proceedings of the Jubilee Conference, Tallahassee, 1978, edited by J. E. Lannutti and P. K. Williams (AIP Conf. Proc. No. 48) (AIP, New York, 1978), p. 112.
[10]In Ref. 8 a smooth transition between the small and large distances was also introduced, but only for the *lower eigenvalue* of the potential matrix. Here we do it for the entire matrix.
[11]J. Lomnitz Adler, V. R. Pandharipande, and R. A. Smith, Nucl. Phys. **A355**, 399 (1981).
[12]M. H. Kalos, Phys. Rev. **128**, 1791 (1962).
[13]M. H. Kalos, D. Levesque, and L. Verlet, Phys. Rev. A **9**, 2178 (1974).
[14]J. Carlson, Phys. Rev. C **36**, 2026 (1987).
[15]D. M. Ceperley and B. J. Alder, J. Chem. Phys. **73**, 3897 (1984).
[16]M. A. Lee, K. E. Schmidt, M. H. Kalos, and G. V. Chester, Phys. Rev. Lett. **46**, 728 (1981).
[17]The suggestion that this family of particles composed of two quarks and two antiquarks be designated with the letter T, which is a capital tau, was made by N. Metropolis on the basis of the Greek word $\tau\epsilon\sigma\sigma\epsilon\rho\alpha$, meaning four.
[18]A. De Rújula, Howard Georgi, and S. L. Glashow, Phys. Rev. D **12**, 1147 (1975).
[19]J. Carlson, J. B. Kogut, and V. R. Pandharipande, Phys. Rev. D **28**, 2807 (1983).